Spectral Properties of the Chalker-Coddington Network

Marcus Metzler and Imre Varga^{1,*}

Department of Physics, Toho University, Miyama 2-2-1, Funabashi, Chiba 274

¹ Institut für Theoretische Physik, Universität zu Köln, Zülpicher Str. 77, D-50937 Köln, Germany

(Received January 21, 2020)

We numerically investigate the spectral statistics of pseudo-energies for the unitary network operator U of the Chalker-Coddington network. The shape of the level spacing distribution as well the scaling of its moments is compared to known results for quantum Hall systems. We also discuss the influence of multifractality on the tail of the spacing distribution.

KEYWORDS: Chalker-Coddington model, level spacing distribution, scaling, quantum Hall systems, multifractality

§1. Introduction

The Chalker-Coddington network model,¹⁾ representing systems of independent two-dimensional (2D) electrons in a strong perpendicular magnetic field and smooth disorder potential, is a convenient tool to investigate the quantum Hall universality class.^{1–3)} It has been used to determine various quantities characterizing the localization-delocalization (LD) transition taking place between the quantized plateaus of the Hall conductance.⁴⁾ The first approach was to use the transfer matrix method to numerically determine the characteristic exponent $\nu \approx 2.35$ for the divergence of the localization length $\xi \propto |E-E_c|^{-\nu}$ when the energy of the electron E approaches the critical energy E_c .^{1,5)} At the critical energy itself the network model was used to calculate critical wave functions. Those were subjected to a multifractal analysis and the critical exponent $\alpha_0 \approx 2.27$ describing the scaling of typical value of their squared amplitude with the system size, $\exp(|\Psi_c|^2) \propto L^{-\alpha_0}$, was determined.²⁾ The model can also very conveniently be used to simulate the diffusion of wave packets using a unitary time evolution operator U. By doing so it was possible to determine the scaling behavior of the local density of states.^{6,7)}

Recently, a new approach in the investigation of network models was suggested. It was argued that network models can be used to determine the statistics of the eigenvalue spectrum of their underlying system by investigating the spectrum of the unitary network operator U.³⁾ So far

^{*} Permanent address: Department of Theoretical Physics, Institut of Physics, Technical University of Budapest, H-1521 Budapest, Hungary

the numerical investigation of the pseudo-energy statistics has been concentrating on the number variance $\Sigma_2(N) = \langle (n - \langle n \rangle)^2 \rangle$ of an energy interval containing on average $N = \langle n \rangle$ levels and the compressibility $\chi = \lim_{N \to \infty} \lim_{L \to \infty} \frac{d\Sigma_2}{dN}$. It was found that the prediction by Chalker et al⁸ that $\chi = (d - D_2)/(2d)$, where D_2 is the correlation dimension, can be confirmed. Furthermore, it was seen that the level spacing distribution function P(s), denoting the probability to find two consecutive levels separated by an energy $\epsilon = s\Delta$, Δ being the average level spacing, deviates in its tail from the Wigner surmise.³ This was expected at the critical energy⁹⁻¹¹ and was also seen in other numerical investigations.¹²⁻¹⁴ In this paper we are going to take a closer look at the level spacing distribution P(s). We will show that by using the spectrum of the unitary network operator U all the known results regarding P(s) can be reproduced. Furthermore, we will introduce an improved numerical method to determine that spectrum by reducing the size of the matrix that has to be diagonalized.

§2. The Network Operator and its quasi energy spectrum

The Chalker-Coddington network is a 2D regular lattice whose nodes consist of elementary scatterers. The scatterers are connected by unidirectional channels. Each scatterer is a 2×2 matrix S^k mapping 2 incoming channel amplitudes onto 2 outgoing channels. In order to simulate random channel lengths, a random kinetic phase is added to each channel amplitude. Vertical links are always scattered to horizontal links and vice versa. The scattering probability to the left and the right are determined by a transmission amplitude T and a reflection amplitude R = 1 - T, respectively. This chiral structure of the network captures the basic features of the motion of 2D electrons in a strong magnetic field and smooth random potential, i.e. the potential correlation length d is much larger than the magnetic length l. In this picture the network links represent the equipotential contours of the random potential and its nodes are the saddle points. The scattering amplitude is determined by the electron energy E and the energy u_k of the respective saddle point, $T = (1 + \exp((E - u_k)/E_t))^{-1}$, where E_t is the characteristic tunneling energy of the potential.^{2,15)} The saddle point energies can be either fixed $(u_k = 0 \text{ for all } k)$ or randomly distributed $(u_i \in [-W, W])$, in any case an LD phase transition occurs when E approaches the critical energy $E_{\rm c}=0.^{1)}\,$ In the following we assume that all saddle points have energy $u_k=0$, i.e. W=0,corresponding to the original Chalker-Coddington model. This is done to avoid effects caused by classical percolation. We will discuss the case W>0 and the corresponding percolation effects in a later publication.

A state or wave function of the network is defined by a normalized vector $\Psi = (\psi_1, \dots, \psi_n)$ whose elements ψ_i denote the complex amplitudes on the $n = 2L^2$ network channels, where L is the system size. Its time evolution is determined by the scattering matrices at the saddle points

which can be incorporated into a single unitary network operator U:

$$\psi_i(t+1) = \sum_{j=1}^{2L^2} U_{ij}\psi_j(t),$$

where the U_{ij} are either appropriately arranged matrix elements of the scattering matrices S^k or zero. This results in U having only two non-zero elements per matrix column and being energy dependent through the energy dependence of the scattering amplitudes. An energy eigenstate Ψ of the underlying electronic system is a solution of the stationarity equation:

$$U(E)\Psi = \Psi, \tag{1}$$

which corresponds to an eigenstate of U(E) with eigenvalue 1. Such an eigenstate will occur only at discrete values of $E = E_n$ which form the energy spectrum of the modeled system. In contrast to these energy eigenvalues, the eigenvalue spectrum of U(E), defined by the equation

$$U(E)\Psi_{\alpha} = e^{i\omega_{\alpha}(E)}\Psi_{\alpha},\tag{2}$$

for a fixed value of E is much easier to determine.²⁾ As was pointed out in Ref. 3, the eigenphases $\omega_{\alpha}(E)$ show the same statistics as eigenenergies E_n close to E. They can be considered an excitation spectrum at energy E and we will refer to them as pseudo-energies.

The fact that we can choose the energy E at which we want to investigate the level statistics makes it possible to look directly at the critical energy E_c without having to worry about leaving the critical region. This means that all the critical pseudo-energies, i.e. the eigenvalues of $U(E_c)$, can be used for our statistics, which is an enormous advantage over other methods that can only use part of the eigenspectrum of their Hamiltonians. In order to further improve the efficiency of the numerics, we also use the fact that for any eigenphase ω_{α} the phase $\omega_{\alpha} + \pi$ is also an eigenphase. This pseudo-degeneracy is caused by the chiral structure of the Chalker-Coddington model and the resulting fact that each time step maps horizontal to vertical links only and vice versa. If you look at U^2 this property results in the formation of two orthogonal U^2 -invariant subspaces that have the same eigenvalues. This U^2 degeneracy is reflected in the pseudo-degeneracy in U, which forced us to disregard half the eigenvalues in the past. Now we will use it to reduce the size of our matrix. When diagonalizing the matrix U^2 , instead of U, and calculating the degenerate eigenphases $2\omega_{\alpha}$, we can take out all matrix elements corresponding to vertical (or horizontal) links and thereby reduce the matrix to a quarter of its size. Diagonalizing this stripped matrix and dividing all its eigenphases by 2 gives us the upper semi-circle of all eigenvalues of U, which is the maximum yield possible, within a much shorter time. Now let us take a look at the results.

§3. The level spacing distribution P(s) and scaling

The level spacing distribution in the localized regime, i.e. at energies $|E| \gg E_c = 0$ is Poissonian: $P_P(s) = \exp(-s)$. The closer we get to the critical energy the more it will change and become closer

to the GUE distribution of the metallic phase known from random matrix theory, $^{16)}$ $P_{GUE}(s) = \frac{32}{\pi^2}s^2 \exp\left(-\frac{4}{\pi}s^2\right)$ (see Fig. 1). Since we do not have a metallic phase in the quantum Hall regime, the GUE distribution will not be reached. At the critical energy the distribution is neither GUE nor Poisson, because the critical wave functions are neither smeared out homogeneously nor are they localized on a small area. Instead, they form a self similar measure fluctuating strongly on all length scales, which is best described in terms of multifractality. It has been found that at criticality the P(s) distribution is best overall fitted by the following formula: 14)

$$P(s) = As^{\beta} \exp\left(-Bs^{\alpha}\right),\tag{3}$$

where A and B are determined by the normalization conditions $\langle 1 \rangle = 1$ and $\langle s \rangle = 1$. This shape was proposed by analytical theories that predicted that $\alpha = 1 + 1/(d\nu) \approx 1.21^{.10,11}$ We will see that this prediction is not supported by our data, instead an earlier prediction for the tail region of P(s) that makes a connection to the compressibility χ can be verified, i.e. $P(s) \propto \exp(-s/(2\chi))$.

In our investigation we determined pseudo-energy spectra for system sizes L ranging from 16 to 50, i.e. L^2 saddle points and eigenvalues per system. The number of realizations per system size was set to get from 4×10^4 up to 5×10^6 eigenvalues. This resulted in enough statistics to get good results for P(s) for values of s up to about s = 4.0. In Fig. 1 P(s) is shown at different energies ranging from $E = E_c = 0$ to E = 3. The change from the critical distribution at E = 0, which does not fit the GUE behavior, to the Poissonian type, which is almost reached at E = 3, can be seen very clearly. This change is expected to show one-parameter scaling for any function Z(E, L) that describes the shape of P(s):

$$Z(E, L) = f(L/\xi), \quad \xi = \xi_0 |E - E_c|^{-\nu}.$$
 (4)

As a scaling variable we consider several quantities, first¹⁹⁾

$$J_0(L, E) = \int_0^\infty Q_0(s)ds = \frac{1}{2} \int_0^\infty s^2 P(s)ds,$$
 (5)

where $Q_0(s)$ is the probability that an energy interval of width s contains no energy eigenvalue. Note that J_0 is half the lowest order momentum of P(s) that is nontrivial and is also connected to $q = \langle s^2 \rangle^{-1}$ that describes the 'peakedness' of a distribution.^{20,21)} Furthermore, we invoke the entropic moment of P(s), $-\langle s \ln(s) \rangle$ and calculate, apart from $-\ln(q)$, another generalized Rényientropy $S_{\text{str}} = -\langle s \ln(s) \rangle + \ln \langle s^2 \rangle$.^{20–22)}

All of these quantities are numerically easily obtainable and they take all calculated neighboring level spacings into account. Since all of them show nice scaling behavior we present only that of J_0 . The inset in Fig. 2 shows J_0 as a function of E for different system sizes. As expected, all the curves meet in a single size independent point $J_0^c = 0.61 \pm 0.01$ at the critical energy $E = E_c = 0$. If we assume the validity of Eq. (4) we can rescale L so that the data points of J_0 as a function of L/ξ for consecutive energies E overlap with each other. The result of such a rescaling is shown in

Fig. 2. In this case we fit a fourth degree polynomial in $\ln(L/\xi_0) + \nu \ln E$ to a log-log plot of our data and thereby determined $\nu = 2.1 \pm 0.3$. This is consistent with other results for ν obtained by various previous studies.^{23–27)}

Now, let us proceed with the shape analysis of the P(s) function using the other two quantities q and $S_{\rm str}$. As it has been shown in a number of cases^{20,22)} these parameters apart from showing scaling and fixed point in the critical regime, as a bonus enable us to determine the one-parameter family of P(s) functions describing the transition from e.g. GUE-like to Poissonian behavior. To this end we apply the same linear rescaling as was done in Ref 21 and introduce \tilde{Q} and \tilde{S} that span the whole [0, 1] interval with 0 (1) corresponding to the Poissonian (GUE-like) limits, respectively. In Fig. 3 the parametric dependence of \tilde{S} vs \tilde{Q} is shown. We clearly see, that all the data fall on a common curve as was already seen in numerical simulation of the random–Landau matrix model. 21) Furthermore, as a comparison, the behavior of the $\tilde{S}(\tilde{Q})$ dependence is also given for three families of P(s) functions based on Eq. (3): a) fixed $\beta = 2$ and variable α in the range [1,2]; b) fixed $\alpha = 1$ and variable β in the range [0,2]; and c) using $\beta = 2\gamma$ and $\alpha = \gamma + 1$ with variable γ in the range [0,1]. The first and the second families meat each other at the "semi-Poissonian" of the form $P(s) = \frac{27}{2}s^2 \exp(-3s)$ similar to that proposed in Ref 9. The family c is a Brody-like form that has already been seen to fit the evolution of the system in the \tilde{S} vs \tilde{Q} parameter space in Ref 21. As we can see our data indicate a similar behavior as the random-Landau matrix model. This is another nice example of the presence of one-parameter scaling since all data can be described by a one-parameter family of P(s) functions. This analysis suggests $\gamma \approx 0.54$ around the critical point (E = 0).

Right at the critical energy, however, the two parameter fit of P(s) to Eq. (3) is shown in Fig. 4. The fit was done for all available system sizes and resulted in the averaged values $\alpha = 1.56 \pm 0.04$ and $\beta = 1.99 \pm 0.03$. The errors were determined by the fitting and averaging procedures. Within those errors the result is almost the same as that obtained by Ono *et al.* for the Landau model in the lowest Landau band¹⁴ ($\alpha = 1.53$, $\beta = 2.19$). This contradicts the prediction that $\alpha = 1.21$.^{10,11}

In Ref 18 it was argued that the tail should show an exponetial decay. The results of a fit to a function $\exp(-\kappa s)$ are shown in the inset of Fig. 4. We get $\kappa = 3.95 \pm 0.6$, which is comparable to the result by Batsch and Schweitzer²⁸ ($\kappa \approx 4.1$) and fits the prediction $\kappa = 1/(2\chi)$, with $\chi = 0.124 \pm 0.06$.³

§4. Conclusion

In conclusion we have presented the statistical analysis of spectra of pseudo-energies taken at different electron energies obtained in a network-model of the quantum-Hall effect. We could confirm that those pseudo-energy spectra show the same statistics as those of the energy eigenvalues of other models of the quantum Hall systems. This was done by investigating the shape of the level spacing distribution function P(s) and the scaling of its moments $J_0 = \langle s^2 \rangle/2$, $q = \langle s^2 \rangle^{-1}$ and

 $-\langle s \ln s \rangle$. Furthermore, although the overall shape of P(s) at the critical point has yet to be explained, we observe that level repulsion leads to the same quadratic behavior for small s as in the metallic regime, whereas the tail of the P(s) distribution falls off more slowly than in the GUE case. This is due to the multifractality of the critical wave functions and is also reflected in the finite compressibility $(0 < \chi < 1)$.

Acknowledgements

We would like to thank M. Janssen and Y. Ono for valuable discussions. Partial support from DFG and SFB-341 as well as OTKA Nos. T021228, T024136, F024135 are gratefully acknowledged.

- 1) J. T. Chalker, P. D. Coddington: J. Phys. C 21(1988) 2665.
- 2) R. Klesse and M. Metzler: Europhys. Lett. 32(1995) 229.
- 3) R. Klesse and M. Metzler: Phys. Rev. Lett. **79**(1997) 721.
- 4) M. Janssen, O. Viehweger, U. Fastenrath, and J. Hajdu: Introduction to the Theory of the Integer Quantum Hall Effect (VCH, Weinheim; New York; Basel; Cambridge; Tokyo, 1994).
- 5) D. H. Lee, Z. Wang, S. Kivelson: Phys. Rev. Lett. **70**(1993) 4130.
- 6) B. Huckestein and R. Klesse: Phys. Rev. B 55(1997) R7303.
- 7) R. Klesse: Ph.D. Thesis, Universität zu Köln, 1996.
- 8) J. T. Chalker, V. E. Kravtsov, I. V. Lerner: JETP Lett. 64(1996) 386.
- 9) B. I. Shklovskii, B. Shapiro, B. R Sears, P. Lambrianides, H. B. Shore: Phys. Rev. B 47(1993) 11487.
- 10) V. E. Kravtsov, I. V. Lerner, B. L. Altshuler, A. G. Aronov: Phys. Rev. Lett. 72(1994) 888.
- 11) A. G. Aranov, V. E. Kravtsov and I. V. Lerner: JETP Lett. **59**(1994) 39.
- 12) D. Braun, G. Montambaux: Phys. Rev. B **52**(1995) 13903.
- 13) S. N. Evangelou: Phys. Rev. B 49(1994) 16805.
- 14) Y. Ono, T. Ohtsuki, B. Kramer: J. Phys. Soc. Jpn. 65(1996) 1734.
- 15) H. A. Fertig: Phys. Rev. B 38(1988) 996.
- 16) M. L. Mehta: Random Matrices, 2nd ed. (Academic Press, New York, 1991).
- 17) M. Janssen: Int. J. Mod. Phys. 8(1994) 943.
- 18) B. L. Altshuler, I. Kh. Zharekeshev, S. A. Kotochigova and B. Shklovskii: JETP 67(1988) 625.
- 19) I. Kh. Zharakeshev and B. Kramer: Jpn. J. Appl. Phys. **34**(1995) 4361.
- 20) I. Varga, E. Hofstetter, J. Pipek, M. Schreiber: Phys. Rev. B 52(1995) 7783.
- 21) I. Varga, Y. Ono, T. Ohtsuki, and J. Pipek: Phys. Status Solidi B 205(1998) 373.
- 22) I. Varga, J. Pipek, M. Janssen, and K. Pracz: Europhys. Lett. 36(1996) 437.
- 23) H. Aoki and T. Ando: Phys. Rev. Lett. 54(1985) 831.
- 24) B. Huckestein and B. Kramer: Phys. Rev. Lett. 64(1990) 1473.
- 25) Y. Huo and R.N. Bhatt: Phys. Rev. Lett. 68(1992) 1375.
- 26) Dongzi Liu and S. Das Sarma: Phys. Rev. B 49(1994) 2677.
- 27) T. Ohtsuki and Y. Ono: J. Phys. Soc. Jpn. 64(1995) 4088.
- 28) M. Batsch and L. Schweitzer: High Magnetic Fields in the Physics of Semiconductors II: Proceedings of the International Conference, Würzburg 1996, edited by G. Landwehr and W. Ossan (World Scientific Publishers Co., Singapure, 1997), pp. 47–50.

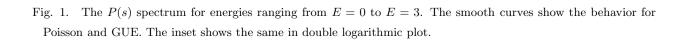


Fig. 2. The one-parameter dependence of the scaling variable J_0 on $L/\xi(E)$. The inset shows J_0 as a function of energy E for different system sizes. At the critical point $E_c = 0$ all the curves meet at the same point.

Fig. 3. The parametric dependence of \tilde{S} vs \tilde{Q} for our numerical results compared to three families of P(s) functions as described in the text.

Fig. 4. The P(s) distribution for $E=E_c=0$. We can see the data for L=20,24,30,40,50. All data points are positioned on the smooth curve that is a fit to Eq. (3), where $\alpha=1.56\pm0.04$ and $\beta=1.99\pm0.03$. The inset shows a fit of $\exp(-\kappa s)$ to the data for L=40, $\kappa=3.95\pm0.06$.

